ЖЭТФ, 2014, том 146, вып. 5 (11), стр. 1002–1013

MAGNETIC STRUCTURE AND DOMAIN CONVERSION OF THE QUASI-2D FRUSTRATED ANTIFERROMAGNET $CuCrO_2$ PROBED BY NMR

Yu. A. Sakhratov [a,b], ***L. E. Svistov*** [c*], ***P. L. Kuhns*** [a], ***H. D. Zhou*** [a,d], ***A. P. Reyes*** [a]

[a] *National High Magnetic Field Laboratory, Tallahassee 32310, Florida, USA*

[b] *Kazan State Power Engineering University 420066, Kazan, Russia*

[c] *Kapitza Institute for Physical Problems Russian Academy Sciences 119334, Moscow, Russia*

[d] *Department of Physics and Astronomy, University of Tennessee, Knoxville 37996, Tennessee, USA*

Received June 17, 2014

We measured ^{63,65}Cu NMR spectra in a magnetic field up to about 15.5 T on a single crystal of the multiferroic triangular-lattice antiferromagnet $CuCrO_2$. The measurements were performed for perpendicular and parallel orientations of the magnetic field with respect to the c-axis of the crystal, and the detailed angle dependence of the spectra on the magnetic field direction in the ab-plane was studied. The shape of the spectra can be well described in the model of spiral spin structure suggested by recent neutron diffraction experiments. When the field is rotated perpendicular to the crystal c-axis, we for the first time directly observed a remarkable reorientation of the spin plane simultaneous with rotation of the incommensurate wavevector, by quantitatively deducing the conversion of the energetically less favorable domain to a more favorable one. At high enough fields parallel to the c-axis, the data are consistent with either a field-induced commensurate spiral magnetic structure or an incommensurate spiral magnetic structure with a disorder in the c direction, suggesting that high fields may have influence on interplanar ordering.

DOI: 10.7868/S0044451014110121

1. INTRODUCTION

The problem of an antiferromagnet on a triangular planar lattice has been intensively studied theoretically [1–5]. The ground state in the Heisenberg and XY models is a "triangular" planar spin structure with three magnetic sublattices arranged 120° apart. The orientation of the spin plane is not fixed in the exchange approximation in the Heisenberg model. The applied static field does not remove the degeneracy of the classical spin configurations. Therefore, the usual small corrections such as quantum and thermal fluctuations and relativistic interactions in the geometrically frustrated magnets play an important role in the formation of the equilibrium state [2, 5, 6]. The magnetic phase diagrams of such two-dimensional magnets strongly depend on the spin value of magnetic ions.

$CuCrO_2$ is an example of the quasi-two-dimensional antiferromagnet ($S = 3/2$) with a triangular lattice structure. Below $T_N \approx 24$ K, $CuCrO_2$ exhibits spiral ordering to an incommensurate spiral magnetic structure with a small deviation from the regular 120° structure. The transition to the magnetically ordered state is accompanied by a small distortion of the triangular lattice. We present an NMR study of the low-temperature magnetic structure of $CuCrO_2$ in the fields up to 15.5 T. These fields are small in comparison with exchange interactions within the triangular plane ($\mu_0 H_{sat} \approx 280$ T). Hence, we can expect that in our experiments, the exchange structure within an individual plane is not distorted significantly and the field evo-

*E-mail: svistov@kapitza.ras.ru

lution of NMR spectra in our experiments is to spin plane reorientation or a change in the interplane ordering. The microscopic properties of magnetic phases of this magnet are especially interesting because this material is multiferroic [7–9]. The possibility to modify electric and magnetic domains with electric and magnetic fields makes $CuCrO_2$ attractive for experimental study of the magnetoelectric coupling in this class of materials.

2. CRYSTAL AND MAGNETIC STRUCTURE

The $CuCrO_2$ structure consists of magnetic Cr^{3+} ($3d^3$, $S = 3/2$), nonmagnetic Cu^+, and triangular O^{2-} lattice planes (TLPs), which are stacked along the c-axis in the sequence Cr–O–Cu–O–Cr (space group $R\bar{3}m$, $a = 2.98$ Å, and $c = 17.11$ Å at room temperature [10]). The respective layer stacking sequences are $\alpha\gamma\beta$, $\beta\alpha\gamma$, and $\beta\beta\alpha\alpha\gamma\gamma$ for Cr, Cu, and O ions. The crystal structure of $CuCrO_2$ projected on the ab-plane is shown in top portion of Fig. 1. The distances between the nearest planes denoted by different letters for copper and chromium ions and the pairs of planes for oxygen ions are $c/3$, whereas the distance between the nearest oxygen planes denoted by the same letters is $(1/3 - 0.22)c$ (Ref. [10]). No structural phase transition has been reported at temperatures higher than the Néel ordering temperature ($T > T_N \approx 24$ K). In the magnetically ordered state, the triangular lattice is distorted, such that one side of the triangle becomes slightly smaller than the other two sides: $\Delta a/a \approx 10^{-4}$ (Ref. [11]).

The magnetic structure of $CuCrO_2$ has been intensively investigated by neutron diffraction experiments [10, 12–15]. It was found that the magnetic ordering in $CuCrO_2$ occurs in two stages [15, 16]. At the higher transition temperature $T_{N1} = 24.2$ K, a two-dimensional (2D) ordered state within ab-planes sets in, whereas below $T_{N2} = 23.6$ K, three-dimensional (3D) magnetic order with the incommensurate propagation vector $\mathbf{q}_{ic} = (0.329, 0.329, 0)$ along the distorted side of TLPs [11] is established. The magnetic moments of Cr^{3+} ions can be described by the expression

$$\mathbf{M}_i = M_1\mathbf{e}_1\cos(\mathbf{q}_{ic}\cdot\mathbf{r}_i+\theta)+M_2\mathbf{e}_2\sin(\mathbf{q}_{ic}\cdot\mathbf{r}_i+\theta), \quad (1)$$

where $\mathbf{e}_1$ and $\mathbf{e}_2$ are two perpendicular unit vectors determining the spin plane orientation with the normal vector $\mathbf{n} = \mathbf{e}_1 \times \mathbf{e}_2$, $\mathbf{r}_i$ is the vector to the ith magnetic ion, and θ is an arbitrary phase. The spin-plane orientation and the propagation vector of the

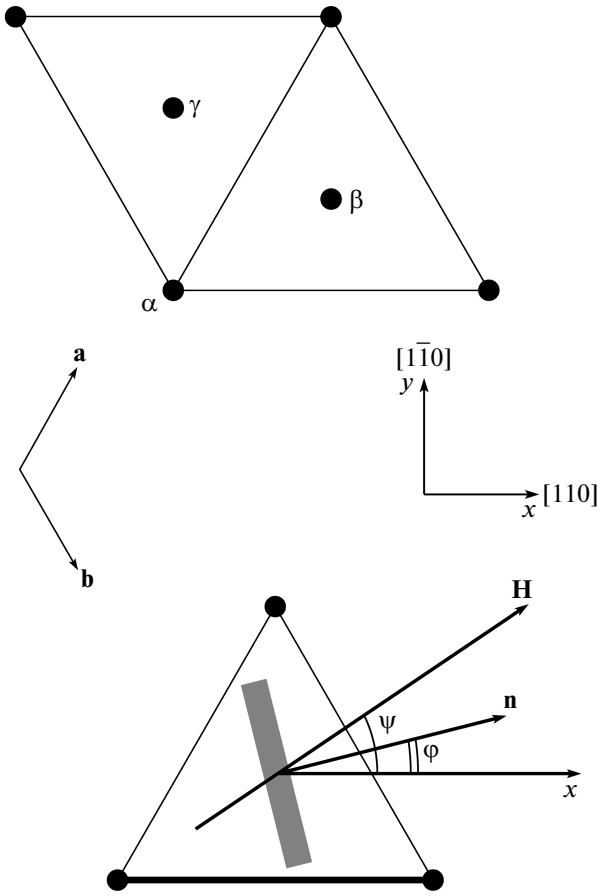

Fig. 1. Top: Crystal structure of $CuCrO_2$ projected on the ab-plane. The three layers, $\alpha\beta\gamma$, are the positions of Cr^{3+} ions. Bottom: Reference angles ψ and φ as defined in the text; the grey bar corresponds to the projection of the spin plane. The incommensurate wavevector $\mathbf{q}_{ic}$ is collinear with the base of the triangle (thick line)

magnetic structure are schematically shown in the bottom of Fig. 1. For a zero magnetic field, $\mathbf{e}_1$ is parallel to [001] with $M_1 = 2.8(2)\mu_B$, while $\mathbf{e}_2$ is parallel to [1$\bar{1}$0] with $M_2 = 2.2(2)\mu_B$ (Ref. [15]). The pitch angle between the neighboring Cr moments corresponding to the observed value of $\mathbf{q}_{ic}$ along the distorted side of the TLP is equal to 118.5° which is very close to 120° expected for the regular TLP structure. Realization of such magnetic structure has the natural explanation in the frame of Dzyaloshinskii–Landau theory of magnetic phase transitions (Ref. [17]).

Owing to the crystallographic symmetry in the ordered phase, we can expect six magnetic domains at $T < T_N$. The propagation vector of each domain can be directed along one side of the triangle and can be

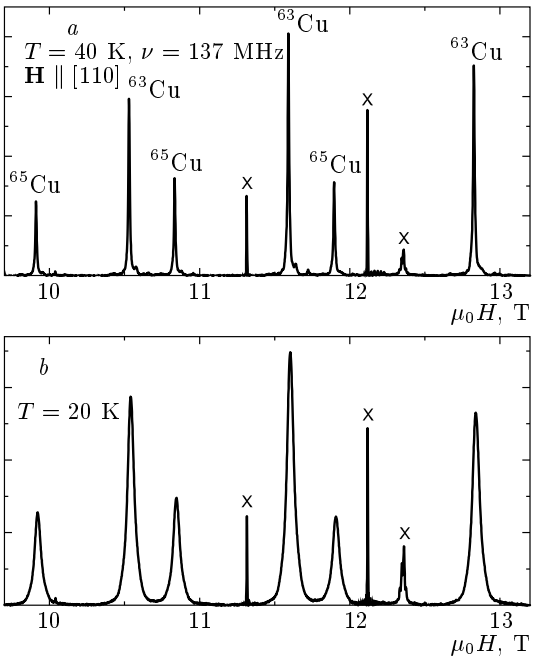

Fig. 2. The ^{63,65}Cu NMR spectra of a $CuCrO_2$ single crystal (a) in the paramagnetic state and (b) in the ordered state at the external magnetic field directed perpendicular to c axis, $\mathbf{H} \parallel [110]$. The two sets of lines correspond to the signals from quadrupolar split ^{63}Cu and ^{65}Cu nuclei. The peaks marked with crosses are spurious ^{63,65}Cu and ^{27}Al NMR signals from the probe

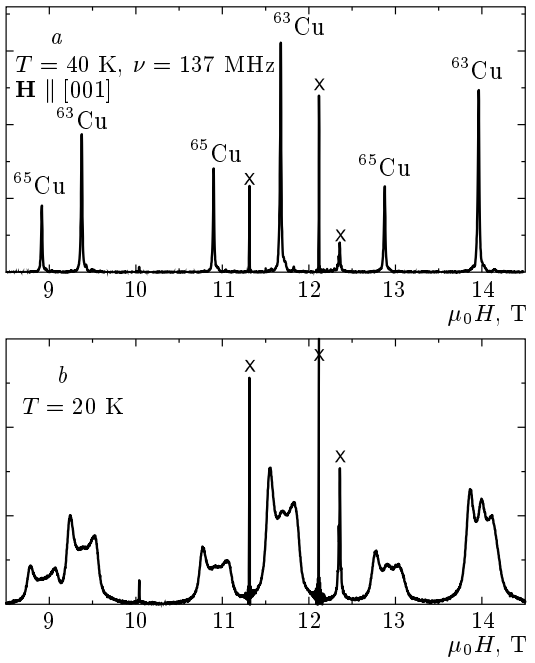

Fig. 3. Spectra similar to those in Fig. 2 but with the field applied parallel to c axis, $\mathbf{H} \parallel [001]$

positive or negative. As reported in Refs. [14, 18], the distribution of the domains is strongly affected by the cooling history of the sample.

Inelastic neutron scattering data [19] have shown that $CuCrO_2$ can be regarded as a quasi-2D magnet. The spiral magnetic structure is defined by the strong exchange interaction between the nearest Cr^{3+} ions within the TLPs with the exchange constant $J_{ab} = 2.3$ meV. The inter-planar interaction is at least one order of magnitude weaker than the in-plane interaction.

Results of the magnetization, ESR, and electric polarization experiments [9, 18] have been discussed in the framework of the planar spiral spin structure at fields studied experimentally: $\mu_0 H < 14$ T $\ll \mu_0 H_{sat}$ ($\mu_0 H_{sat} \approx 280$ T). The orientation of the spin plane is defined by the biaxial crystal anisotropy. One hard axis for the normal vector $\mathbf{n}$ is parallel to the c direction and the second axis is perpendicular to the direction of the distorted side of the triangle. The anisotropy along the c direction dominates, with the anisotropy constant approximately hundred times larger than that within the ab-plane resulting from distortions of the triangle structure. A magnetic phase transition was observed for the field applied perpendicular to one side of the triangle ($\mathbf{H} \parallel [1\bar{1}0]$) at $\mu_0 H_c = 5.3$ T, which was consistently described [9, 14, 18] by the reorientation of the spin plane from (110) ($\mathbf{n} \perp \mathbf{H}$) to ($1\bar{1}0$) ($\mathbf{n} \parallel \mathbf{H}$). This spin reorientation occurs due to weak susceptibility anisotropy of the spin structure $\chi_{\parallel} \approx 1.05\chi_{\perp}$.

3. SAMPLE PREPARATION AND EXPERIMENTAL DETAILS

A single crystal of $CuCrO_2$ was grown by the flux method following Ref. [15]. The crystal structure was confirmed by single-crystal room-temperature X-ray spectroscopy. The magnetic susceptibility $M(T)/H$ was measured at $\mu_0 H = 0.5$ T in the temperature range 2–300 K using a SQUID magnetometer. The obtained susceptibility curve χ_c was similar to the data in Refs. [8, 20]. The Néel temperature $T_N \approx 24$ K and the Curie–Weiss temperature $\theta_{CW} = -204$ K obtained from the fitting of $M(T)$ at temperatures 150 K $< T <$ 300 K are in agreement with the values given in Ref. [8].

NMR experiments were carried out using a home-built NMR spectrometer. Measurements were taken

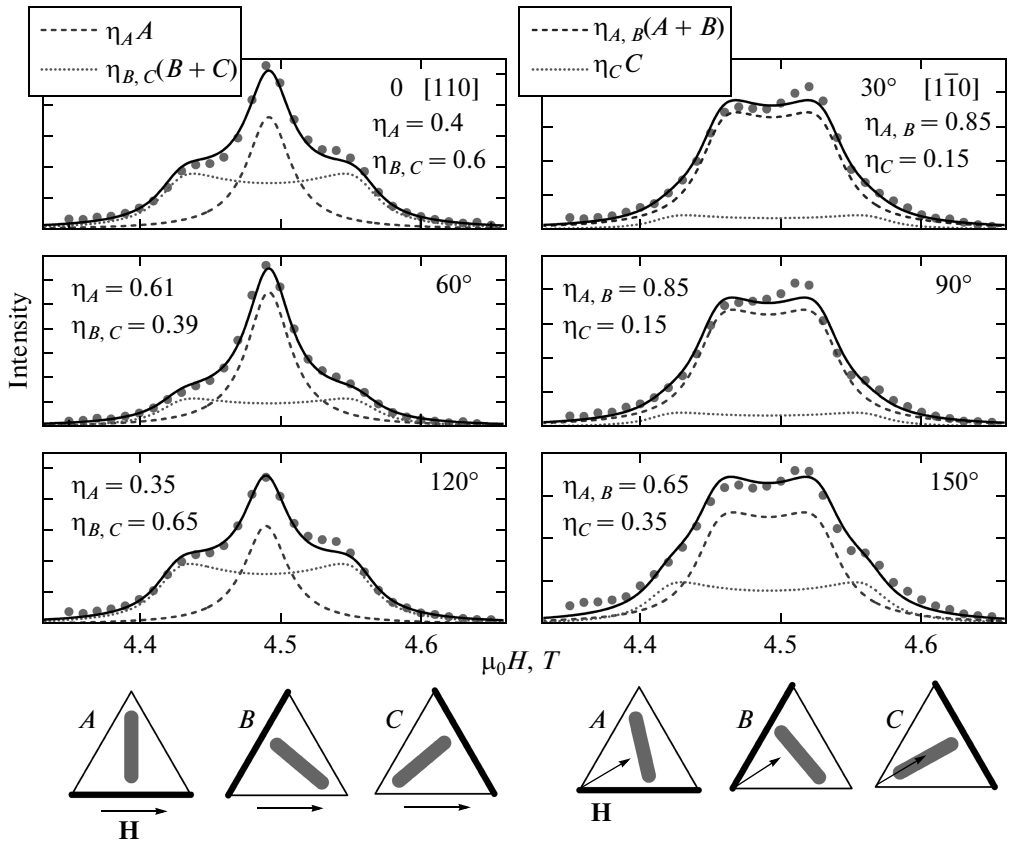

Fig. 4. The ^{63}Cu NMR spectra ($m_I = -1/2 \leftrightarrow +1/2$) measured at different angles between **H** applied within the ab-plane and the [110] direction of the sample (solid circles). ZFC to $T = 20$ K and $\nu = 55.3$ MHz. Solid lines are the calculated spectra in the model of the magnetic structure (Eq. (1)) and orientations of spin planes (grey bars) shown in the bottom of the figure. A, B, and C correspond to three possible alignments of the propagation vector of the magnetic structure ($\mathbf{q}_{ic}$ is collinear to the triangle side marked thick); η_A, η_B, η_C are the relative weights of the NMR signals from A, B, C domains, which were used for the best coincidence with experiment

on a 17.5 T Cryomagnetics field-sweepable NMR magnet at the National High Magnetic Field Laboratory. The ^{63,65}Cu nuclei (nuclear spins $I = 3/2$, gyromagnetic ratios $\gamma^{63}/2\pi = 11.285$ MHz/T and $\gamma^{65}/2\pi = 12.089$ MHz/T) were probed using the pulsed NMR technique. In the figures that follow, the spectra shown by solid lines were obtained by summing fast Fourier transforms (FFT), while the spectra shown by circles were obtained by integrating the averaged spin-echo signals as the field was swept through the resonance line. The NMR spin echoes were obtained using 1.5 μs–τ_D–3μs ($\mathbf{H} \parallel \mathbf{c}$), 1.8 μs–τ_D–3.6 μs ($\mathbf{H} \perp \mathbf{c}$, $\mu_0 H \sim 4.5$ T), and 2.3 μs–τ_D–4.6 μs ($\mathbf{H} \perp \mathbf{c}$, $\mu_0 H \sim 11.6$ T) pulse sequences, where the respective times between pulses τ_D were 15, 20, and 15 μs. Measurements were carried out in the temperature range 4.2 K $\leq T \leq$ 40 K stabilized with a precision better than 0.03 K. The experimental setup allowed rotating the sample inside the excitation coil with respect to the static field $\mathbf{H} \perp \mathbf{c}$ during the experiment.

4. EXPERIMENTAL RESULTS

The ^{63,65}Cu NMR spectra for the paramagnetic (Figs. 2a, 3a) and ordered (Figs. 2b, 3b) states for $\mathbf{H} \perp \mathbf{c}$ and $\mathbf{H} \parallel \mathbf{c}$ consist of two sets of lines, corresponding to ^{63}Cu and ^{65}Cu isotopes. Each set consists of three lines: one of them corresponds to the central line ($m_I = -1/2 \leftrightarrow +1/2$) and two quadrupole satellites correspond to ($\pm 3/2 \leftrightarrow \pm 1/2$) transitions.

For the paramagnetic state, the spectral shape was found to be independent of the magnetic field orientation in the ab-plane. By contrast, the shapes of the

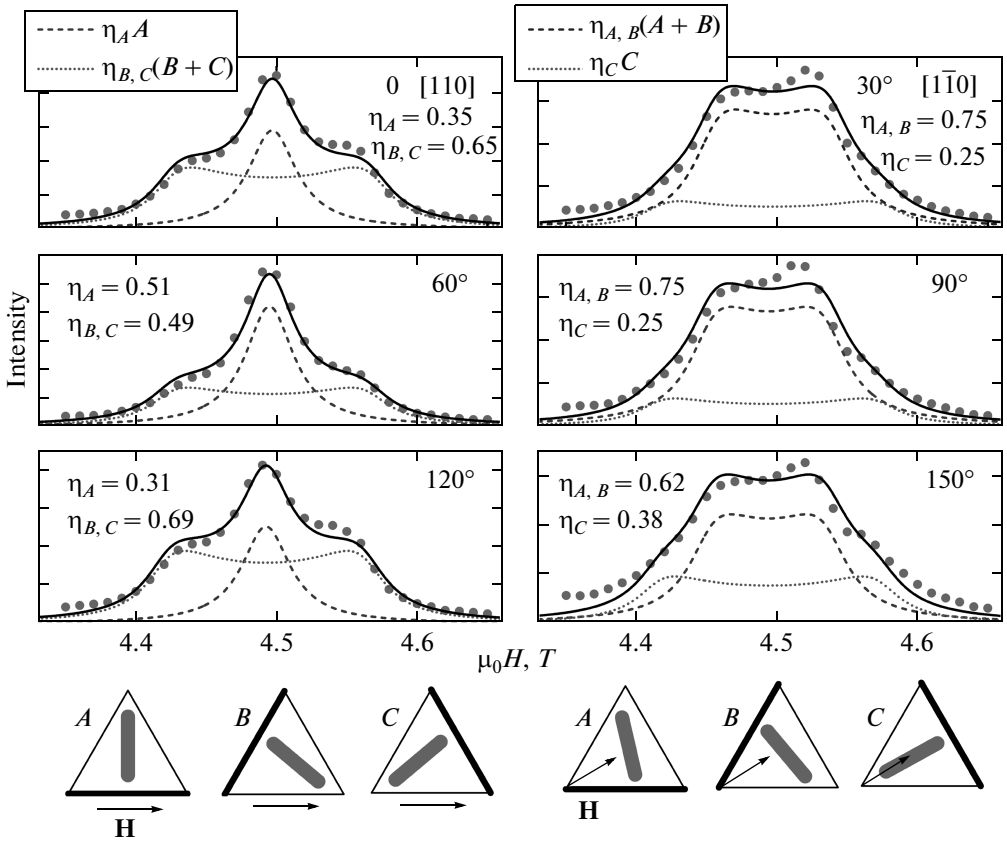

Fig. 5. Data similar to those in Fig. 4 but for ZFC to $T = 4.2$ K

spectra at temperatures below T_N are strongly dependent on the field direction and cooling history. The spectra were studied under two cooling conditions: zero field cooling (ZFC) and field cooling (FC).

In the first set of the experiments, the static field was oriented within the *ab*-plane (Figs. 4–9). The static magnetic field during the FCs was directed parallel (**H** ∥ [110]) or perpendicular (**H** ∥ [1$\bar{1}$0]) to one side of the triangular structure. For all FC data, the sample was cooled in a field of 16.9 T from 40 to 4.2 K (or 5 K) with the characteristic time $t_{cooling} \approx 40$ min, and then the measurements were performed. The sample was rotated about the *c*-axis. The direction of the external field given in the figures is measured with respect to the [110] direction of the sample. Because the data obtained for the full rotation of the sample reveal a 180° symmetry, only data from 0 to 150° are shown for clarity.

The angular dependences in the *ab*-plane were measured at the frequencies 55.3 MHz and 137 MHz. The lower frequency is chosen such that the central line of ^{63}Cu NMR is situated at fields near 4.5 T, i. e., below the reorientation field $\mu_0 H_c = 5.3$ T, whereas the higher frequency places the resonance above $\mu_0 H_c$.

The NMR spectra were measured at two temperatures $T_{high} = 20$ K (Figs. 4 and 8) and $T_{low} = 4.2$ K (Figs. 5, 6, 7) and $T_{low} = 5$ K (Fig. 9). We chose these two temperature sets, because the domain walls in $CuCrO_2$ are mobile at high temperatures, whereas at low temperatures the walls are pinned [18].

In the second set of the experiments, the static field was oriented parallel to the *c* direction. Representative ZFC spectra at 20 K measured at different fields are shown in Fig. 10.

5. DISCUSSION

We discuss the results of the NMR experiments in the framework of the planar spiral spin structure (Eq. (1)) proposed from neutron diffraction experiments [15] and carried out at $H = 0$. The spin plane orientation of such a structure is defined by weak relativistic interactions with the external field and crystal

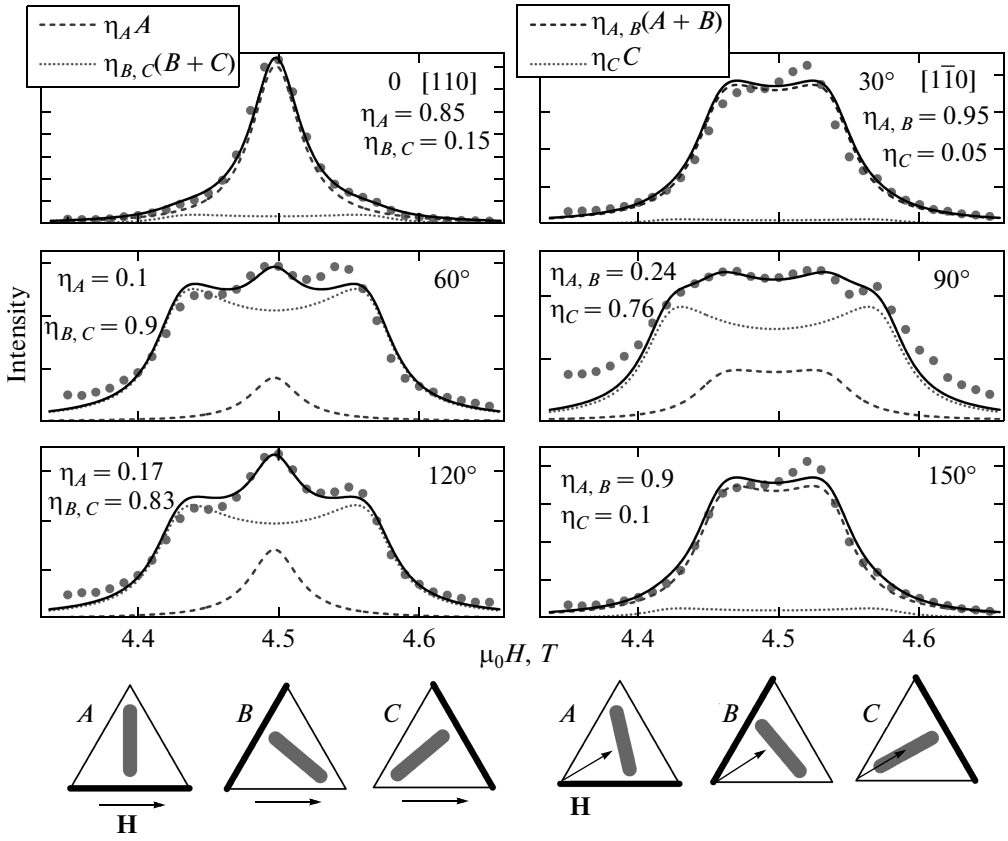

Fig. 6. Data similar to those in Fig. 4 but for FC $\mathbf{H}(16.9\ \mathrm{T}) \| [110]$ ($\psi = 0$) to $T = 4.2$ K. The background in some panels is due to the overlap with ^{65}Cu NMR lines

environment. Following Ref. [18], the anisotropic part of the magnetic energy of $CuCrO_2$ can be written as

$$U = -\frac{\chi_\parallel - \chi_\perp}{2}(\mathbf{n}\cdot\mathbf{H})^2 + \frac{A}{2}n_z^2 + \frac{B}{2}n_y^2, \qquad (2)$$

where $A > B > 0$. For an arbitrary field direction in the ab-plane, the vector $\mathbf{n}$ monotonically rotates from $\mathbf{n} \| [110]$ to $\mathbf{n} \| \mathbf{H}$. This can be defined by minimizing Eq. (2), which can be rewritten as

$$U = -\frac{\Delta\chi}{2}H^2\left(\cos^2(\psi-\varphi) - \left(\frac{H_{cy}}{H}\right)^2\sin^2\varphi\right) + \frac{A}{2}n_z^2. \qquad (3)$$

Here, the angles ψ and φ define the directions of the respective vectors $\mathbf{H}$ and $\mathbf{n}$, as depicted in Fig. 1. Using the reorientation field value $\mu_0 H_{cy} = 5.3$ T, we obtain the expected orientations of the spin planes relative to the field directions of our NMR experiments. For the field directed along the "thick" side of the triangle in the ab-plane (i. e., $\psi = 0$), $\varphi = 0$ at all fields. For the field directed along the "thin" side of the triangle (i. e., $\psi = 60°$), the expected angles φ for a given field are $\varphi(\mu_0 H = 4.5\ \mathrm{T}) = 22.15°$ and $\varphi(\mu_0 H = 11.6\ \mathrm{T}) = 54.3°$. For the field direction perpendicular to the "thick" side of the triangle (i. e., $\psi = 90°$), $\varphi(\mu_0 H < \mu_0 H_{cy} = 5.3\ \mathrm{T}) = 0$ below spin-flop and $\varphi(\mu_0 H > \mu_0 H_{cy} = 5.3\ \mathrm{T}) = 90°$ above spin-flop. For the field direction perpendicular to the "thin" side of the triangle (i. e., $\psi = 30°$), the spin plane orientation is defined by the angles $\varphi(\mu_0 H = 4.5\ \mathrm{T}) = 12.3°$ and $\varphi(\mu_0 H = 11.6\ \mathrm{T}) = 25.4°$.

For $\mathbf{H} \| \mathbf{c}$, the field of spin reorientation transition H_{cz} is expected to be much larger than the fields in our experiments [18]. We therefore expect the spin plane orientation for $\mathbf{H} \| \mathbf{c}$ to be the same as at $H = 0$ ($\mathbf{n} \| [110]$).

Analyzing the NMR spectral shapes, we found that they can be well described within the spiral spin structure model given by Eq. (1) with the incommensurate propagation vector directed along one side of the triangle, $\mathbf{q}_{ic} = (0.329, 0.329, 0)$. Generally, the local mag-

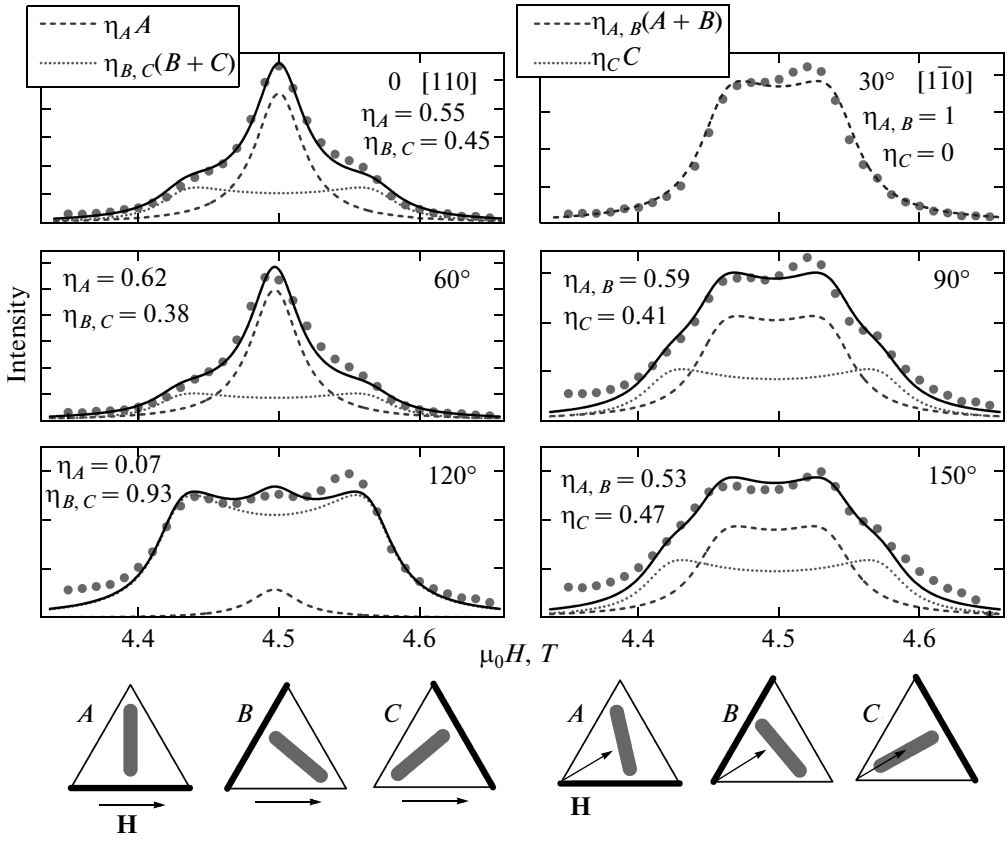

Fig. 7. Data similar to those in Fig. 4 but for FC $\mathbf{H}(16.9\ \mathrm{T}) \| [1\bar{1}0]$ ($\psi = 30°$) to $T = 4.2$ K. The background in some panels is due to the overlap with ^{65}Cu NMR lines

netic field at Cu sites is the sum of the long-range dipole field $\mathbf{H}_{dip}$ and the transferred hyperfine contact field produced by the nearest Cr^{3+} moments. The ^{63,65}Cu NMR of $CuCrO_2$ in the paramagnetic state was studied in Ref. [21], where it was shown that the effective field at the copper site is proportional to the chromium moment with a hyperfine field of 3.3 T/μ_B. This value does not depend on the direction of the chromium moment. The computed dipolar fields on the chromium nuclei in the paramagnetic phase are anisotropic and essentially smaller than experimentally observed, and are respectively equal to 0.17 T/μ_B and -0.08 T/μ_B for $\mathbf{H} \| [001]$ and $\mathbf{H} \| [1\bar{1}0]$. From these data, we presume that the effective field measured in the paramagnetic phase [21] is mostly defined by the contact fields from six nearest chromium magnetic ions. Although the contact field created by an individual neighboring chromium moment ($(1.3/6)$ $\mathrm{T}/\mu_B = 0.55$ T/μ_B) is much larger than the dipole field, dipolar and contact hyperfine contributions prove to be comparable in the ordered state. This is due to a strong compensation of the contact fields from the six nearest chromium moments in the ordered state. We took both contributions into account in our calculations. The dipolar fields on the copper nuclei were computed by numerically summing contributions from nearest-neighbor Cr moments in the sphere of the radius 20 Å; accounting for the moments farther away gives no noticeable effect. The shape of the individual NMR line was taken Lorentzian for the fits.

The best fit with experiment for $\mathbf{H} \perp \mathbf{c}$ was obtained with the value of Cr^{3+} magnetic moments $M_1 = M_2 = 0.91(5)\mu_B$ at low fields $\mu_0 H \sim 4.5$ T (Figs. 4, 5, 6, 7) and $M_1 = M_2 = 1.15(9)\mu_B$ at high fields $\mu_0 H \sim 11.6$ T (Figs. 8, 9). Each individual linewidth is $\delta = 20(5)$ mT for all fitted NMR spectra. This value is consistent with the linewidth measured in the paramagnetic phase.

Since the copper nuclei in $CuCrO_2$ are situated at a position of high symmetry, the NMR spectra from the magnetic domains with opposite directions of incommensurate vectors $+\mathbf{q}_{ic}$ and $-\mathbf{q}_{ic}$ are identical. In the analysis that follows, we assign the magnetic domains the letters A, B, and C, having in mind that each let-

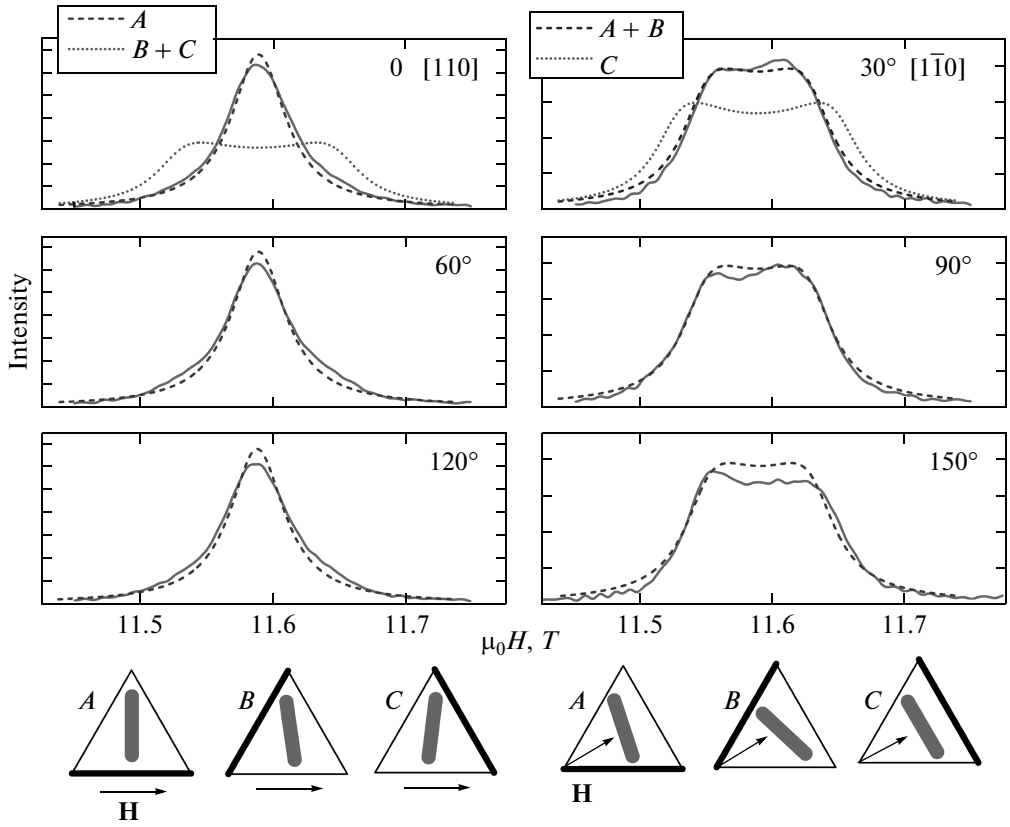

Fig. 8. Data similar to those in Fig. 4 but for ZFC to $T = 20$ K, $\nu = 137$ MHz

ter refers to two magnetic domains indistinguishable by the NMR method.

The ZFC NMR spectra measured at the frequency 55.3 MHz and temperatures 20 K and 4.2 K are shown in Figs. 4 and 5. For the field directed parallel to one side of the triangle ($\psi = 0$, 60°, 120°), we expect the resonance conditions of two domains (B, C) to be equivalent. A sketch of the expected spin-plane orientations within A ($\psi = 0$, $\varphi = 0$), B ($\psi = 60°$, $\varphi = 22.15°$), and C ($\psi = 120°$, $\varphi = 157.85°$) domains are shown at the bottom left of each figure. The dashed and dotted lines respectively show the computed spectra for domains A and $B + C$. The resulting spectrum was obtained by summing the spectra from the three domains with relative weights η_A, η_B, η_C and is shown with solid lines in the figures.

If the relative sizes of the domains do not change during the rotation of the field, we expect that the sum of the relative fractions η_A of domain A measured at three unique orientations $\psi = 0$, 60°, 120°, i. e., $\eta_A(0)+\eta_A(60°)+\eta_A(120°)$, is equal to unity. The same is true for the sum $\eta_C(30°)+\eta_C(90°)+\eta_C(150°)$. However, the experimental values of the sums at $T = 20$ K (Fig. 4) are $\eta_A(0) + \eta_A(60°) + \eta_A(120°) = 1.36$ and $\eta_C(30°) + \eta_C(90°) + \eta_C(150°) = 0.65$. This deviation from unity shows that the domain sizes of the sample change with field rotation. These observations show that the size of the energetically favorable domains grows at the expense of unfavorable domains. To our knowledge, this phenomenon is directly observed for the first time via the NMR technique.

For measurements at $T = 4.2$ K (Fig. 5), the sums are closer to unity: $\eta_A(0) + \eta_A(60°) + \eta_A(120°) = 1.17$ and $\eta_C(30°) + \eta_C(90°) + \eta_C(150°) = 0.88$. This implies that the mobility of domain walls increases with the temperature. We emphasize that the conversion of the domain structure implies changes not only in the spin plane orientation but also in the direction of the wave vector $\mathbf{q}_{ic}$.

The field cooling of the sample enables us to prepare the sample with the energetically preferable domains. If the field during the cooling process was directed along one side of the triangle ($\psi = 0$, Fig. 6), domain A is preferable. In this case, field-cooling the sample results

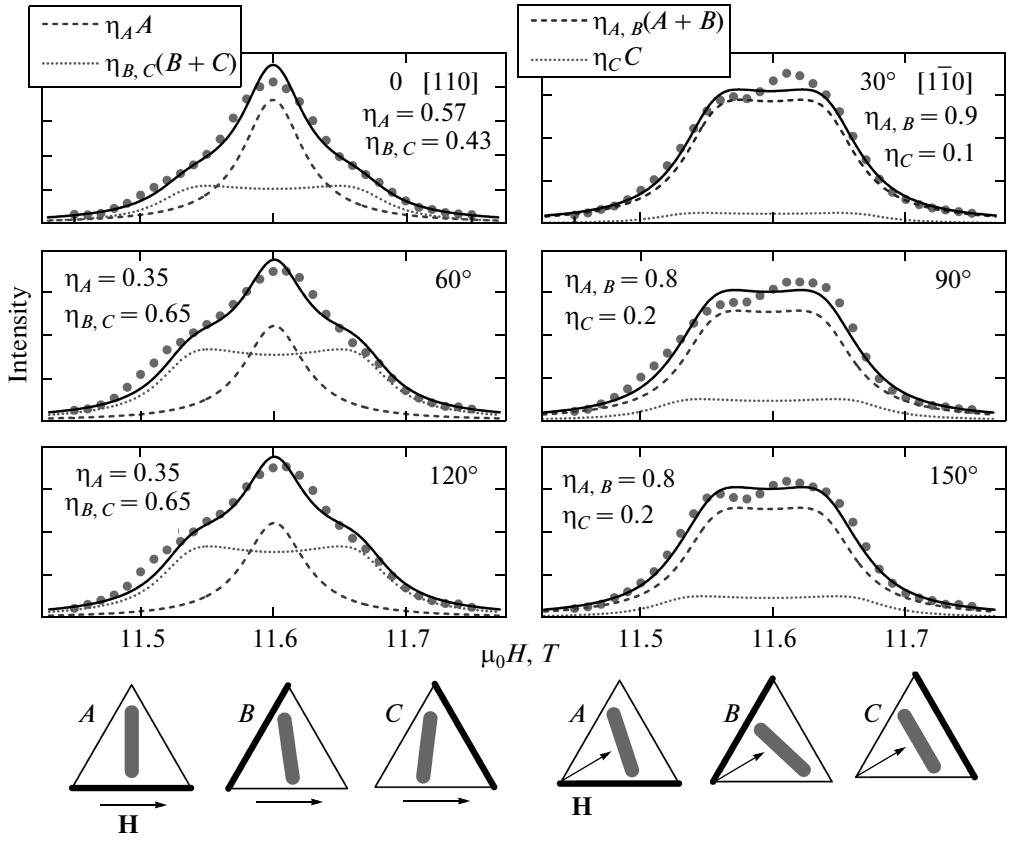

Fig. 9. Data similar to those in Fig. 4 but for ZFC to $T = 5$ K, $\nu = 137$ MHz

in an approximately 85 % domain A and approximately 15 % B and C. If the cooling field is directed perpendicular to one side of the triangle ($\psi = 30°$, Fig. 7), domains B and C are preferable. In that case, the NMR signal from the unfavorable domain is negligibly small and the two other domains have nearly the same sizes. Interestingly, the relative part of the sample where the direction of $\mathbf{q}_{ic}$ changes with field rotation at $T = 4.2$ K has nearly the same intensity as for the ZFC procedure. The parameters defining the domain conversion for FC samples are $\eta_A(0) + \eta_A(60°) + \eta_A(120°) = 1.12$ and $\eta_C(30°) + \eta_C(90°) + \eta_C(150°) = 0.91$ for the cooling field direction $\psi = 0$ (Fig. 6). For the cooling field direction $\psi = 30°$ (Fig. 7), these parameters are respectively 1.24 and 0.88. Thus, the domain conversion during the rotation of the static field $\mu_0 H \approx 4.5$ T at $T = 4.2$ K occurs within 4–8 % of the sample.

Such domain conversion is more clearly observed at higher fields $\mu_0 H \approx 11.6$ T $> \mu_0 H_c = 5.3$ T and a higher temperature $T = 20$ K (see Fig. 8). For the fields directed along one side of the triangular structure, the NMR spectra can be solely identified with a single energetically preferable domain with $\mathbf{q}_{ic}$ parallel to the applied field ($\psi = 0$, 60°, 120°, spectra in the left panels of Fig. 8). This means that at $T = 20$ K, the field (approximately 11.6 T) not only rotates the spin plane of the magnetic structure but also rebuilds the domain structure, such that only the energetically preferable domains are established in the sample, namely, the domains with $\mathbf{q}_{ic} \parallel \mathbf{H}$. For the fields directed perpendicular to one side of the triangle ($\psi = 30°$, 90°, 150°, spectra in the right panels of Fig. 8), domains A and B are more energetically preferable. The ZFC spectra observed at high fields (approximately 11.6 T) and low temperature (5 K) (Fig. 9) are qualitatively similar to ZFC spectra measured at low fields (approximately 4.5 T). Only the sums defining the domain conversion of the sample, $\eta_A(0) + \eta_A(60°) + \eta_A(120°) = 1.27$ and $\eta_C(30°) + \eta_C(90°) + \eta_C(150°) = 0.5$, are larger than those for the low field (1.17 and 0.88, respectively).

The NMR spectra measured at the field directed along the c-axis (hard axis for the $\mathbf{n}$ vector of the structure) is 2.5 times broader than those with fields aligned within the ab-plane, Fig. 10. The shape of the spec-

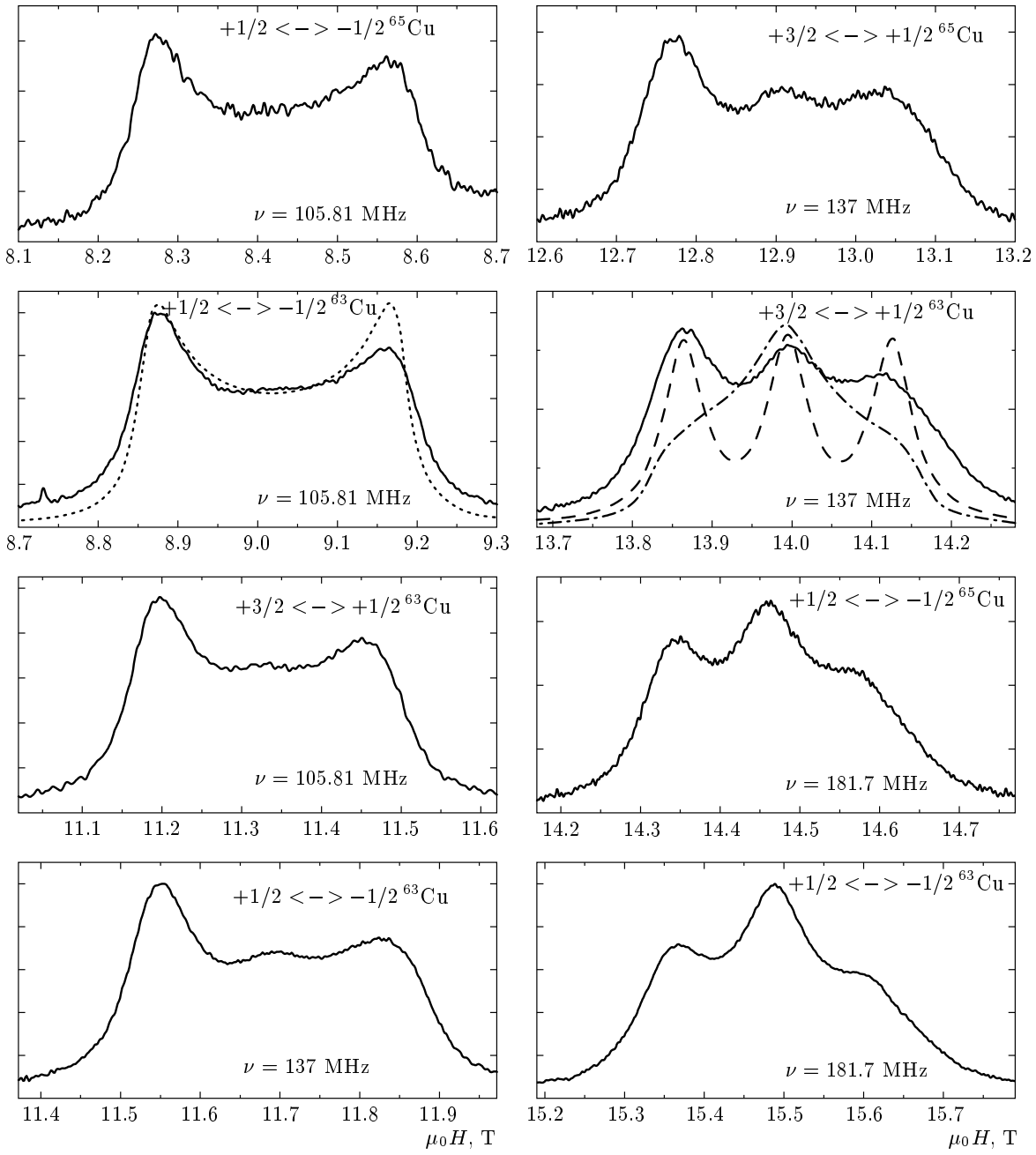

Fig. 10. Representative ^{63,65}Cu NMR spectra at different fields (solid lines) under the ZFC condition, $T = 20$ K. Shown are data taken with each field swept over a narrow range at fixed frequencies. The x axis was adjusted such that each panel covers the same field range. The dotted line is the spectrum calculated using Eq. (1), dot-dashed and dashed lines are the calculated spectra corresponding to the incommensurate spiral magnetic structure with disorder in the c direction and the commensurate spiral magnetic structure

tra depends on the field value. In the low-field range ($\mu_0 H \lesssim 10$ T), the shape has two horns similar to those observed for fields oriented within the ab-plane. For higher fields, an additional third peak appears in the middle of the spectra.

The low-field spectra can be satisfactorily described by the model of incommensurate spiral spin structure similar to the structure proposed for zero field (Eq. (1)). The best fit at $T = 20$ K and $\mu_0 H \approx 9$ T is obtained with $M_1 = M_2 = 2.1\ \mu_B$ and $\delta = 20$ mT (Fig. 10, the

dotted line).

The change of the NMR spectral shape at higher fields indicates the field evolution of the magnetic structure. We suggest two possible models of the high-field magnetic structure. The dash-dotted line in Fig. 10 shows the NMR spectra computed using Eq. (1) with random phases θ for structures within different triangular planes with $M_1 = M_2 = 2.2\ \mu_B$ and $\delta = 20$ mT. This model accounts for the incommensurate spiral magnetic structure within every ab-plane with disorder in the c direction. In this case, the experimental spectra can be described by the sum of the spectra from the parts of the sample with order and disorder along the c direction.

Another model for the three-horn spectra is the commensurate magnetic structure with the pitch angle close to 120°, in which one moment looks along $[00\bar{1}]$ direction, i. e., opposite to the applied field **H**. The NMR spectrum computed in that case with $M_1 = M_2 = 2.7\ \mu_B$ and $\delta = 30$ mT is shown in Fig. 10 with the dashed line. A transition of the spiral structure from incommensurate to commensurate in large enough fields has been observed in other compounds with a triangular structure [22–24].

For both models, the values of M_1 and M_2 are closer to the maximum value expected for the chromium magnetic moment $g\mu_B S$, compared to those values for the perpendicular orientation. It is probable that the static field applied along the c direction suppresses the fluctuating part of the magnetic moments of Cr ions, which could explain its large value for $\mathbf{H} \parallel \mathbf{c}$ compared to its value for $\mathbf{H} \perp \mathbf{c}$.

The observed "third peak" peculiarity possibly corresponds to a phase transition also seen by recent electric polarization experiments [25].

6. CONCLUSIONS

The ^{63,65}Cu NMR spectra measured at $\mathbf{H} \perp [001]$ can be well described by the planar spiral magnetic structure with the oscillating components of the moments approximately 2.5 times smaller than those obtained from neutron diffraction experiments [10, 15]. Rotation of the sample in a magnetic field results in the reorientation of the spin plane accompanied by reorientation of the incommensurate wave vector of the structure. This wave vector follows the direction of the magnetic field at high enough temperature and fields, whereas at low temperatures or low fields, the propagation vector is defined by the cooling history of the sample. The results are consistent with previous results for electric polarization and with ESR studies [9, 18].

The NMR study of the magnetic structure at $\mathbf{H} \parallel [001]$ shows that the low-field magnetic structure is consistent with the structure suggested by neutron diffraction experiments. In fields higher than 10 T, the magnetic structure is modified. The results can be described by the loss of long-range ordering in the c direction, or by the transition from the incommensurate to commensurate structure. This observation opens interesting possibilities for future experimental investigations.

We thank V. I. Marchenko and V. L. Matukhin for the stimulating discussions. Yu. A. S. is grateful to the Institute of International Education, Fulbright Program, for financial support (Grant 68435029). H. D. Z. is grateful for the support from NSF-DMR through award DMR-1350002. This work was supported by the RFBR, Program of Russian Scientific Schools (Grant 13-02-00637). Work at the National High Magnetic Field Laboratory is supported by the NSF Cooperative Agreement No. DMR-0654118, and by the State of Florida.

REFERENCES

1. H. Kawamura and S. Miyashita, J. Phys. Soc. Jpn. **54**, 4530 (1985).
2. S. E. Korshunov, J. Phys. C: Sol. St. Phys. **19**, 5927 (1986).
3. P. W. Anderson, Science **235**, 1196 (1987).
4. M. L. Plumer and A. Caille, Phys. Rev. B **42**, 10388 (1990).
5. A. V. Chubukov and D. I. Golosov, J. Phys.: Condens. Matter **3**, 69 (1991).
6. E. Rastelli and A. Tassi, J. Phys.: Condens. Matter **8**, 1811 (1996).
7. S. Seki, Y. Onose, and Y. Tokura, Phys. Rev. Lett. **101**, 067204 (2008).
8. K. Kimura, H. Nakamura, K. Ohgushi, and T. Kimura, Phys. Rev. B **78**, 140401(R) (2008).
9. K. Kimura, H. Nakamura, S. Kimura, M. Hagiwara, and T. Kimura, Phys. Rev. Lett. **103**, 107201 (2009).
10. M. Poienar, F. Damay, C. Martin, V. Hardy, A. Maignan, and G. Andre, Phys. Rev. B **79**, 014412 (2009).

11. K. Kimura, T. Otani, H. Nakamura, Y. Wakabayashi, and T. Kimura, J. Phys. Soc. Jpn. **78**, 113710 (2009).

12. H. Kadowaki, H. Kikuchi and Y. Ajiro, J. Phys.: Condens. Matter **2**, 4485 (1990).

13. M. Soda, K. Kimura, T. Kimura, M. Matsuura, K. Hirota, J. Phys. Soc. Jpn. **78**, 124703 (2009).

14. M. Soda, K. Kimura, T. Kimura, and K. Hirota, Phys. Rev. B **81**, 100406(R) (2010).

15. M. Frontzek, G. Ehlers, A. Podlesnyak, H. Cao, M. Matsuda, O. Zaharko, N. Aliouane, S. Barilo, S. V. Shiryaev, J. Phys.: Condens. Matter **24**, 016004 (2012).

16. O. Aktas, G. Quirion, T. Otani, and T. Kimura, Phys. Rev. B **88**, 224104 (2013).

17. V. I. Marchenko, Zh. Eksp. Teor. Fiz. **146**, №12 (2014).

18. A. M. Vasiliev, L. A. Prozorova, L. E. Svistov, V. Tsurkan, V. Dziom, A. Shuvaev, Anna Pimenov, and A. Pimenov, Phys. Rev. B **88**, 144403 (2013).

19. M. Poienar, F. Damay, C. Martin, J. Robert, and S. Petit, Phys. Rev. B **81**, 104411 (2010).

20. T. Okuda, N. Jufuku, S. Hidaka, and N. Terada, Phys. Rev. B **72**, 144403 (2005).

21. A. G. Smolnikov, V. V. Ogloblichev, A. Yu. Yakubovsky, Yu. V. Piskunov, S. V. Verkhovskii, A. P. Gerashenko, K. N. Mikhalev, K. Kumagai, and S. Barilo, in *Proc. of the XIV International Youth Scientific School*, Kazan, June 20–25 (2011), p. 65.

22. I. M. Vitebskii, O. A. Petrenko, S. V. Petrov, and L. A. Prozorova, JETP **76**, 178 (1993).

23. S. S. Sosin, L. A. Prozorova, and M. E. Zhitomisrsky, Pis'ma v Zh. Eksp. Teor. Fiz. **79**, 104 (2004).

24. M. Kenzelmann, G. Lawes, A. B. Harris, G. Gasparovic, C. Broholm, A. P. Ramirez, G. A. Jorge, M. Jaime, S. Park, Q. Huang, A. Ya. Shapiro, and L. A. Demianets, Phys. Rev. Lett. **98**, 267205 (2007).

25. Eundeok Mun, M. Frontzek, A. Podlesnyak, G. Ehlers, S. Barilo, S. V. Shiryaev, and Vivien S. Zapf, Phys. Rev. B **89**, 054411 (2014).